# The Role of Activated Carbon Surface on Catalytic Wet Peroxide Oxidation

**Ana Rey, Marisol Faraldos and Ana Bahamonde***

*Instituto de Catálisis y Petroleoquímica, CSIC. C/ Marie Curie Nº 2, 28049 Madrid, Spain*

**José A. Casas, Juan A. Zazo and Juan J. Rodríguez**

*Área de Ingeniería Química, Facultad de Ciencias, Universidad Autónoma de Madrid, Campus de Cantoblanco, 28049 Madrid, Spain*

* To whom correspondence should be addressed, Tel./fax: +34-915854760. E-mail: abahamonde@icp.csic.es

**Abstract**

Three activated carbons with fairly different characteristics have been checked in Catalytic Wet Peroxide Oxidation (CWPO) using phenol as model compound for the purpose of learning on the role of these materials which can be used as supports for the preparation of Fe or other metallic catalysts. A complex contribution of mixed effects is involved making difficult to predict the behaviour of a given activated carbon. The surface of these materials promotes the undesirable decomposition of $H_2O_2$ to un-reactive $O_2$ instead of $^{\bullet}OH$ radicals in an extent depending on the nature and accessibility of the oxygen groups. A frankly basic surface including groups such as pyrone with an egg-shell type distribution on the carbon particle seems to be beneficial for a more effective decomposition of $H_2O_2$ leading to a higher oxidation activity. The presence of iron in the activated carbon ashes is also an important factor which may hide in part other effects derived from the structure and surface composition of the carbon. However, that factor can not explain by itself the differences found in the behaviour of the activated carbons since two of them with a similar Fe content showed markedly different activity in CWPO of phenol.

## 1. Introduction

Activated carbons (AC), a common ingredient in hundreds of environmental applications are well known universal adsorbents both in liquid and gas phases.[1] However, nowadays the fulfillment of severe quality standards is claimed, especially for those substances exerting toxic effects on the environment. In this context methods such as adsorption by activated carbons, are not sufficient to deal with the increasingly stringent environmental demands. Treatments by traditional non-catalytic chemical processes,[2] such as wet air oxidation, or incineration are too energy intensive and thus are restricted to waste effluents with high organic loads. Therefore, new advanced options based on catalytic processes point at being an important goal in wastewater treatments with lower organic contents, being specially promising the so-called Advanced Oxidation Processes (AOPs),[3] which usually operate at or near ambient temperature and pressure. The use of heterogeneous catalysts can substantially improve the efficiency of those processes.

Activated carbons have been used in heterogeneous catalytic processes because they can act as direct catalysts or they can satisfy most of the desirable properties required for a suitable catalytic support. Among their excellent properties can be emphasized their high surface area, well developed porous structure and variable surface composition which determine important differences in their reactivity. In particular, activated carbon-based catalysts have been introduced in some wastewater treatments like catalytic wet air oxidation (CWAO)[4,5] and catalytic wet peroxide oxidation (CWPO).[6,7] The use of AC materials in CWAO requires the process to be conducted at temperatures lower than 423 K and P<10 atm to minimize oxidation of the own activated carbon[8]. AOPs based on ambient near conditions appear more attractive for the introduction of activated carbons as catalysts or catalytic supports and thus, CWPO is a promising emerging technique for the treatment of wastewaters containing recalcitrant pollutants.[9-11]

The present work is centered on the study of the role of the activated carbon surface in CWPO at mild conditions such as atmospheric pressure and 323 K of temperature. Phenol has been used as target compound and three activated carbons of fairly different characteristics have been examined. The decomposition of $H_2O_2$ as well as the evolution of phenol, TOC and oxidation intermediates have been followed for the purpose of learning more in deep on the potential application of activated carbon-supported catalysts in CWPO.

## 2. Experimental

### *2.1. Activated carbons*

Three commercial activated carbons (AC) have been used: CM, produced by Merck (Ref. 102514), with a particle size dp = 1.5 mm and apparent density 0.48 $g \cdot cm^{-3}$; CN, Norit Row 0.8 Supra, an extruded carbon supplied by Norit, with apparent density 0.39 $g \cdot cm^{-3}$ and particle size < 0.6 mm, and finally, CC, a granular activated carbon cod. Centaur HSL manufactured by Chemviron Carbon, with an average particle size 0.8-1 mm and apparent density 0.555 $g \cdot cm^{-3}$.

From CN three other carbon samples were prepared: CN_N was obtained upon heat treatment at 1173 K for 4 hours in $N_2$ atmosphere. CN_HCl was the result of treating CN with 3 M HCl solution at room temperature for seven hours (2 g AC/20 mL HCl solution). Following the sample was washed with distilled water until neutral pH and dried overnight at 353 K. Heating CN_HCl at 1173 K for 4 hours in nitrogen atmosphere, CN_HCl_N was obtained.

### *2.2. Characterization*

Elemental analyses were performed by an Elemental Analyzer LECO CHNS-932. Semi-quantitative Chemical analysis was performed by inductively coupled plasma (OES-ICP) with a Perkin Elmer Optima 3300DV Model. Besides, a semi-quantitative

chemical analysis at $\lambda$ = 165-782 nm by ICP-EOS was carried out trying to identify the elements present in the activated carbon ashes.

Thermal gravimetry and differential temperature analysis (TG-DTA) were performed with a Mettler Toledo TGA/STD A 851e using the following conditions: air flow of 250 $cm^3 \cdot min^{-1}$ at a heating rate of 10 $K \cdot min^{-1}$ from room temperature to 1273 K.

The specific surface area ($S_{BET}$) values, were obtained from nitrogen adsorption-desorption at 77 K using a Micromeritics Tristar apparatus on samples previously outgassed overnight at 523 K to a vacuum of $<10^{-4}$ Pa in order to ensure a dry clean surface free from any loosely held adsorbed species. The specific surface areas were determined by application of the BET equation at relative pressures between 0.02–0.15. The values of the micropore volume and external surface area were calculated from the corresponding t-plots drawn from the adsorption data, and the mesopore volumes were determined from the amount adsorbed at a relative pressure of 0.96 on the desorption branch of the isotherm (equivalent to the filling of all pores below 50 nm width), minus the micropore volume previously determined from the t-method.

The characterization of the porous structure was completed by mercury intrusion porosimetry (MIP) using CE Instruments Pascal 140/240 and applying the Washburn equation. It is assumed a cylindrical non-intersecting pore model, with the values recommended by the IUPAC of 414 K and 484 $mN \cdot m^{-1}$, for the contact angle and surface tension of mercury, respectively; this provides data corresponding to pores from about 300 μm down to 7.5 nm diameter. Total pore volume was evaluated combining both techniques.

The pH of aqueous slurries of activated carbon samples was measured by mixing 0.5 g of AC with 10 mL of $CO_2$-free distilled water kept in a bottle at room temperature and continuously stirred until the pH of the slurry was stabilized.

Photoelectron spectra (XPS) were obtained with a VG Escalab 200R spectrometer equipped with a hemispherical electron analyzer (pass energy of 20 eV) and a Mg K$\alpha$ ($h\nu$ = 1254.6 eV, 1 eV=$1.6302 \cdot 10^{-19}$ J) X-ray source, powered at 120 W. The binding

energies were calibrated relative to the C 1s peak from carbon of the samples at 284.6 eV. For the analysis of the peaks a Shirley type background was used. Peaks were adjusted to a combination of Gaussian and Lorentzian functions using the XPSPeak 4.1 software.

The nature of oxygen surface groups was accomplished by temperature programmed desorption analysis under $N_2$ (TPD-$N_2$). A sample of 0.1 g was placed in a vertical quartz tube under nitrogen flow of 1000 $cm^3 \cdot min^{-1}$ at a heating rate of 10 $K \cdot min^{-1}$ from room temperature to 1173 K. The evolved CO and $CO_2$ were continuously analyzed and determined by using a NDIR analyzer (Siemens Ultramat 23). Peaks deconvolution and analysis were adjusted to Gaussian function by Peakfit 4.12 software.

*2.3. Catalytic activity tests*

CWPO runs were carried out in batch in 50 mL glass bottles at 323 K and initial pH of 3, atmospheric pressure, and the following initial concentrations: 100 $mg \cdot L^{-1}$ of phenol and 500 $mg \cdot L^{-1}$ of $H_2O_2$, corresponding to the theoretical stoichiometric amount to completely oxidize phenol to $CO_2$ and $H_2O$. Powdered activated carbon ($d_{particle}$<100 μm) was added at a concentration of 0.5 $g \cdot L^{-1}$. Phenol adsorption runs were simultaneously performed at the same operating conditions without $H_2O_2$ addition.

Phenol and aromatic oxidation intermediates were analyzed by means of HPLC (Varian Pro-Start 335 Diode array detector) with a Nucleosil C-18 column at 313 K and 20:80 Methanol: Acid Water (0.1 % Acetic acid) as mobile phase at flow 0.8 $mL \cdot min^{-1}$. Short-chain organic acids were analyzed by Ion Chromatograph with chemical suppression (Metrohm 790 IC) using a Metrosep A supp 5-250 column with 3.2 mM:1 mM $Na_2CO_3$:$NaHCO_3$ as mobile phase. Total Organic Carbon (TOC) was measured with an OI TOC Analyzer (TOC-Usch Shimadzu). Hydrogen Peroxide concentration and iron in solution were determined by colorimetric titration with an UV 2100 Shimadzu UV/Vis spectrophotometer using the titanium sulfate and o-phenantroline[12] methods, respectively.

## 3. Results and Discussion

### *3.1. Physicochemical Characterization Studies*

Activated carbons have a porous structure, usually with a relatively small amount of chemically bonded heteroatoms (mainly oxygen and hydrogen)[13]. The AC studied here are essentially constituted by C with H and N in small amounts, as it can be seen in Table 1 where their elemental analyses are summarized. Some significant differences can be observed, being the most important the oxygen content of the CC carbon and the ash content of the CN one compared with the rest. These CN ashes consist essentially of silica alumina, traces of Mg, Ca and K and a certain amount of Fe representing 0.2 % by weight of activated carbon.

It is generally accepted that the average structure of activated carbons consists of aromatic sheets and strips, often bent and resembling a mixture of wood shavings and crumpled paper, with variable gaps of molecular dimensions between them, these being micropores.[14] Of course, the highly disorganized structure of these materials is always dependent on the precursor and on its treatment. Whereas the common structure of graphite consists of hexagonal arrays of carbon atoms that are arranged in layer planes (graphite layer planes) stacked in a special configuration[15]. In activated carbons (amorphous carbon), the hexagonal graphene layers are not in alignment as they are in graphite, they are randomly rotated with respect to each other so there is no three-dimensional order, thus the random ordering of imperfect aromatic sheets results in incompletely saturated valences and unpaired electrons, and this will influence the reactivity and adsorption behavior of these materials.

Two distinct types of sites on graphite-type structures can be thought: the basal plane sites, which are associated with the carbons forming the surface of the layer planes, and the edge sites, which involve the terminal sites of the basal planes. The basal plane sites are relatively inactive, whereas edge planes are the usual chemical/electrochemical active sites.[16] These active sites, which are surface sites capable of dissociatively chemisorbing oxygen, are present in carbon and they are

primarily associated with edge sites or defects in the carbon structure.[17,18] This observation suggests that electrochemical and chemical properties of carbonaceous materials should be influenced by the relative fraction of the active sites. Then, it should be possible, to gain a better understanding of the relationship among their physical properties, chemical reactivity and electrochemical performance by studying their thermal oxidation behaviour.[19]

In Table 2 are given the thermal parameters obtained from TG-DTA in air flow for all these AC materials, where $T_i$ is the ignition temperature,[15] $T_{15}$ is the temperature at which 15 % carbon weight loss takes place and $T_M$ is the temperature corresponding to a maximum in DTA diagram (not shown here).

Different values of the air-TG characteristic temperatures are observed. These differences suggest different ordering and sizes of domains of graphene layers in the configuration of these activated carbons. Since CM shows the highest values of the thermal parameters it may have a higher ordering in its carbon disordered structure.[15] On the opposite, CC presents more disorganized structure and it can be expected to have a higher amount of active sites associated with the edge plane sites and defects. These sites are associated with higher densities of unpaired electrons, which could favour or catalyse chemical reactions like $H_2O_2$ decomposition, or advanced oxidation processes (AOPs) studied here and consequently playing a significant role.

Figure 1(a) shows the nitrogen adsorption-desorption isotherms of the activated carbons. Whereas CC shows a typical type I isotherm characteristic of microporous materials, some hysteresis loops, belonging to type H4, can be seen in CM and CN.

Table 3 summarizes the characterization of the porous structure of the activated carbons. Micropore areas, with values around 900-1000 $m^2 \cdot g^{-1}$ corroborate that their porous structures are governed by microporosity. With regard to the pore volumes and pore size distributions, some important differences are noticed as can be seen in Table 3 and Figure 1(b). Though microporosity is in the three cases the main contribution to the total porosity, a significant presence of meso and macropores can be also seen,

except in the case of CC. The CN carbon shows the most developed porous structure which, in principle, permits to consider it as a better candidate to be used as catalytic support for liquid-phase applications.

To learn on the acid or basic character of the surface of these three activated carbons, Table 3 includes the pH values of their aqueous slurries. These values suggest a slight acidic character of CC (6.2), a certain basic character for CM (8.1) and an important basic character of CN surface (10.4). This parameter may give a good indication about the nature of the surface oxygen complexes and the electronic surface charges of these carbons, since it can be assimilated to the pH at the point of zero charge (PZC) of the solid.[20]

The amount and nature of oxygen surface groups are by far the most important factor affecting the surface characteristics and final behaviour of activated carbon materials in chemical reactions. Generally as the quantitative analysis of the surface functional groups is not straightforward, different techniques, such as XPS or TPD-$N_2$, are used to asses the chemical nature of the oxygen surface groups in activated carbons.

XPS is a surface technique which will provide an estimate of the chemical composition of the few uppermost layers of the material. To learn on the composition of the most external surface of these activated carbons, XPS spectra in the C (1s), O (1s) spectral regions were obtained for all the samples and are shown in Figures 2(a) and 2(b) respectively. Carbonaceous materials, like the ones used in this work, give rise to a peculiar line-shape asymmetrically broadened to C1s spectrum whose intensity decreases very slowly on the high binding energy side indicating a contribution of oxygen-containing functional groups.[21,22] The C(1s) spectrum (Figure 2(a)) has been deconvoluted in five symmetric peaks of the Gaussian type[23] for the three activated carbons. Besides a main peak at 284.5 eV, corresponding to graphitic carbon, the spectrum can be fitted to three more peaks centered at 286.0, 287.0 and 288.5 eV that can be associated with C-O bonds of functional groups such as phenol and/or ethers, with a C=O bond, as in the carbonyl group, and with a –COO- bond characteristic of

carboxylic, anhydride and/or ester groups. Finally, the last peak centered at higher energy, 290.5 eV, is associated with the inter-band peak, corresponding to $\pi \rightarrow \pi^*$ transitions.

Figure 2(b) represents the O(1s) XPS spectra. Each spectrum has been deconvoluted in five symmetric peaks. The first fitted peak at 530.0 eV can be associated to oxygen in the inorganic matter (O-II). The following four peaks, at 531.5, 532.9, 533.9 and 536.0 eV, have been assessed to C=O bonds characteristic of carbonyl and/or quinone groups; with C-O bonds characteristic of phenol, lactone, anhydride and/or ether groups; with COOH corresponding to carboxylic group and to adsorbed water, respectively.[24-26]

The relative concentrations of surface groups obtained from deconvolution of C(1s) and O(1s) XPS regions are summarized in Table 4, where no important differences can be observed among the three AC.

Temperature-programmed desorption in $N_2$ flow also provides information on the nature of the carbon-oxygen groups which decompose upon heating by releasing CO and $CO_2$ at different temperatures. Figure 3 shows the TPD curves of the three activated carbons. The total amounts of CO and $CO_2$ evolved, as obtained by integration of the areas under the curves are indicated in each case. The assessment of surface oxygen groups was performed according to literature criteria.[25,27,28] The results are given in Table 5.

The CM carbon shows the lowest oxygen content, both in terms of CO and $CO_2$ releasing groups. In contrast with the XPS results, now significant differences can be observed between the three activated carbons with respect to the relative distribution of oxygen groups. Whereas CM presents a single peak undoubtedly corresponding to carboxylic acid in the $CO_2$ curve, a more complex distribution was found for CN and CC although the main contribution corresponds to carboxylic acid group as well.

From the CO-TPD curves two main contributions were found in the three carbons assessed to phenol and carbonyl groups. A third lower peak was only detected in CN and CC assigned to anhydride groups.

Three ideal models can be drawn to describe the macroscopic distribution of oxygen surface groups in an activated carbon particle: egg-shell, uniform and egg-yolk. A comparison of the O/C surface and bulk atomic ratios can serve to learn on that distribution. The bulk O/C atomic ratio is obtained from elemental analysis whereas XPS and TPD refer to surface composition. Nevertheless, it is important to consider the limitations of these two techniques. XPS does not reach more than a few nanometers and TPD can be affected by mass-transfer limitations in narrow micropores.

In the case of CM the $O/C_{BULK}$ and $O/C_{XPS}$ ratios present almost the same values suggesting that oxygen is uniformly distributed on the surface. However, the $O/C_{TPD}$ ratio is much lower than the $O/C_{BULK}$ indicating that only a part of the oxygen groups were desorbed by TPD. Given that CM shows the highest micropore volume of the series, it seems reasonable to conclude that its oxygen surface groups are placed in the inner micropores in a significant extent.[29]

In the case of CN, since $O/C_{XPS}$ is higher than $O/C_{BULK}$, a higher density of oxygen groups may be distributed in the most external surface. Besides, it seems that the oxygen surface groups can be completely desorbed as reveals the comparison of bulk and TPD O/C ratios. Consistently, this activated carbon presents the higher meso and macropore volumes so that it can be reasonably concluded that the oxygen surface groups are mainly distributed in the most external surface, approaching to an egg-shell type of distribution.

Finally the CC carbon shows a slightly higher $O/C_{BULK}$ ratio than the $O/C_{XPS}$ suggesting that its oxygen surface groups are more or less uniformly distributed on the surface. Its porous structure is governed by microporosity and part of the oxygen surface groups are not desorbed by TPD-$N_2$, given that the $O/C_{TPD}$ ratio is lower than $O/C_{BULK}$. An

intermediate sharing between uniform and egg-yolk distributions can be assessed for the oxygen groups.

Therefore, these activated carbons show some important differences that can serve to provide useful information on the role of the support when studying the behavior of activated carbon-supported catalysts in CWPO.

*3.2.- Results of CWPO experiments*

The advanced oxidation processes are characterized by a common chemical feature: the capability of exploiting the high reactivity of •OH radicals in driving oxidation processes which are suitable for achieving effective abatement of even less reactive pollutants. It has been longer demonstrated that activated carbon materials can decompose hydrogen peroxide at different operating conditions,[30] which is essential for AOPs like the CWPO process here investigated. It has been assumed that decomposition of $H_2O_2$ by activated carbon involves primarily the exchange of a surface hydroxyl group with a hydrogen peroxide anion, according to Bansal et al.[1] The surface peroxide formed is regarded as having an increased oxidation potential and thus decomposes another $H_2O_2$ molecule releasing oxygen and regenerating the activated carbon site. Besides along direct decomposition reaction, $H_2O_2$ can be activated on the AC surface involving the formation of free radicals, where activated carbon supports can be considered to work as an electron-transfer catalyst similar to the Haber-Weiss mechanism known from the Fenton reaction with the reduced (AC) and oxidized ($AC^+$) catalyst states.[31]

Several studies in the literature have shown that many activated carbons are active for the oxidation of organic pollutants with $H_2O_2$ establishing that the superposition of several effects such as the enhancement of the redox potential of $H_2O_2$ (and the resulting reactive oxygen species) at lower acid pHs[9-11] as well as possible changes in the chemical properties of the AC surface could well be the responsible of oxidizing the organic matter in aqueous medium.

Previous experiments relative to direct hydrogen peroxide decomposition led always to complete conversion after 2-4 hours with the three AC investigated at the operating conditions used in this work. From literature studies it can be assumed that $H_2O_2$ decomposition reaction follows a first-order rate equation with respect to hydrogen peroxide concentration.[30]

In Table 7 are summarized the values of the first order rate constant for direct $H_2O_2$ decomposition obtained with the three activated carbons. Quite different values can be observed depending on the activated carbon. Consequently, this can markedly affect to their behaviour in CWPO.

Figure 4 shows the results obtained in phenol oxidation with $H_2O_2$ using the activated carbons investigated. The evolution of phenol is presented in terms of total organic carbon (TOC) and the $H_2O_2$ conversion curves are also included. Significant differences in $H_2O_2$ conversions along CWPO of phenol can be observed between the three AC. Again, the $H_2O_2$ decomposition rates exhibit the same trend found in the direct hydrogen peroxide decomposition experiments (CM<CN<CC).

For the sake of discrimination between adsorption and reaction, the adsorption curves obtained in absence of $H_2O_2$ are represented. As can be seen, in the case of CC carbon, the adsorption and oxidation curves are coincident thus indicating that oxidation is negligible, at least in terms of mineralization (complete oxidation up to $CO_2$ and $H_2O$). Neither aromatic intermediates nor organic acids were detected in the reaction medium confirming that oxidation reactions are not taking place. Nevertheless, this carbon is the one providing a higher rate of decomposition of $H_2O_2$. These results suggest that the CC carbon provokes a rapid decomposition of hydrogen peroxide to $O_2$ and $H_2O$ instead to the reactive $^{\bullet}OH$ radicals.

On the other side, the CN carbon leads to some significant TOC removal upon oxidation increasing as $H_2O_2$ decomposition proceeds. So, there must be certain active sites in the CN Carbon capable to activate hydrogen peroxide decomposition producing reactive free hydroxyl radicals, which are not present or accessible in the CC carbon.

At this point it is important to recapitulate the main differences between these two carbons. The CC carbon has a higher amount of oxygen surface groups but the amount of $CO_2$-evolving groups is higher for the CN carbon. These groups correspond mostly to carboxylic acid in the case of CC whereas CN shows a more heterogeneous composition, with an important contribution of anhydride and pyrone groups. Moreover, the porous structure of the CC carbon is almost completely microporous whereas the CN one has an important contribution of mesopores with an egg-shell type of distribution of the oxygen groups making them more accessible. The frankly basic character of the CN surface in contrast with the acidic to neutral $pH_{slurry}$ of the CC carbon and the possible presence of some metallic impurities can be also important factors to consider. In fact, the CN carbon yielded an almost double percentage of ash content than the two others and these ashes include Fe in a 0.2 % of the activated carbon weight as indicated before. It is well known that Fe catalyzes the oxidation reactions with $H_2O_2$ (Fenton process). The use of activated carbon-supported Fe catalysts has been described in the literature.[7] Nevertheless the amount of Fe in the CN carbon is far below the concentrations commonly used in Fenton oxidation and CWPO. Moreover, the Fe content of the CC carbon amounts 0.15 % of its weight and the oxidation activity of this activated carbon is almost negligible. Thus, although the effect of Fe can not be disregarded it should not be considered as the determining factor capable to explain the different activities observed for the activated carbons investigated.

It is known that phenol oxidation proceeds through a complex reaction scheme giving rise to some intermediates before mineralization is reached.[32,33] Several intermediates, mainly aromatic and low weight organic acids were always detected when working with the CN carbon. Catechol, hydroquinone and p-benzoquinone were the primary oxidation products as a result of phenol hydroxylation. These aromatic intermediates went through further oxidation to yield short-organic acids before final oxidation to $CO_2$ and $H_2O$. The evolution of phenol and oxidation intermediates is shown in Figure 5.

*3.3.- Study of modified activated carbons*

To learn more in deep on the causes of the different oxidation activity shown by the activated carbons, some modifications were carried out on the surface composition of CN (the one showing a higher activity) and the behaviour of the resulting modified carbons was checked.

In a first approach a treatment with hydrochloric acid was carried out to remove or reduce its ash content. The resulting sample was identified as CN_HCl. Besides, heat-treatment in $N_2$ atmosphere for removing surface oxygen groups was applied to the original and HCl-treated carbons giving rise to CN_N and CN_HCl_N samples, respectively.

Firstly, an important reduction in ash content, from 8.35 % to 2.60 %, was observed after the HCl treatment and the Fe content of the resulting activated carbon was as low as 0.07 %. On the other hand, a decrease of surface area and total pore volume was observed in all the modified carbons (see Table 3). With regard to the $pH_{slurry}$, it decreased to a frankly acidic value after the HCl treatment recovering to a basic value upon heat treatment, although substantially below to that of the original CN carbon. Heating this original carbon increased its basic character (see Table 3).

A significant reduction of the amounts of $CO_2$ and CO evolved upon TPD-$N_2$ was observed for all the modified carbons, including that submitted only to HCl treatment without further heating, as can be seen in Table 8.

The changes on the composition of the CN carbon did not show a remarkable effect on the rate of $H_2O_2$ decomposition in presence or absence of phenol, as can be seen from the results reported in Table 9. With regard to the activity for phenol oxidation, it decreases somehow after heat treatment of the original carbon indicating that some of the lost oxygen groups were active in promoting $^{\bullet}OH$ formation from $H_2O_2$. Nevertheless, in the case of the HCl-treated carbon, the decrease of activity becomes significantly more noticeable, revealing that the Fe leached from the original ashes

must have a significant influence on the oxidation activity. This effect seems to be more important than the corresponding to the oxygen groups since the loss of them upon heating (CN_HCl_N sample) barely affects to the TOC conversion due to oxidation (after subtracting the adsorption contribution).

Another important feature affecting to the oxidation activity seems to be the basic or acidic character of the carbon surface. The HCl-treated carbon has a frankly acidic $pH_{slurry}$ opposite to de original CN carbon.

## 4. Conclusions

The comparison of three commercial activated carbons with fairly different characteristics in CWPO of phenol has revealed that a complex ensemble of mixed effects must be considered when trying to explain the role of the carbon support on the activity of Fe or other metallic catalyst eventually prepared with this type of support. The surface of activated carbon promotes $H_2O_2$ decomposition to non-reactive $O_2$ instead of to $^{\bullet}OH$ radical in an extent depending on the amount and nature of oxygen groups and their accessibility. A frankly basic surface with pyrone groups in a well developed porosity giving rise to an egg-shell type distribution on the carbon particles seems to be beneficial. Nevertheless, the presence of Fe in the ash fraction seems to have some significant effect which may hide in part the true influence of the oxygen surface groups, although this effect can not explain by itself the differences shown on the activities of the activated carbons since two of them having similar Fe contents yielded markedly different activities.

## Acknowledgement

We gratefully acknowledge the Spanish Ministry of Education and Science by the financial support of the CTQ2007-61748/PPQ, CTQ2005-02284/PPQ and CTM2007-60577/TECNO projects, and Norit and Chemivon companies for their generous supplying of the activated carbon materials in this research work. The authors also

thank Professor J. L. G. Fierro for his help in the AC characterization studies by XPS. Ana Rey wishes to acknowledge a FPU grant from the Spanish Ministry of Education and Science.

**Literature Cited**

(1) Bansal, R. C.; Donnet, J. B.; Stoeckli, F. *Active Carbon*; Marcel Dekker: New York, 1998.

(2) Andreozzi, R; Caprio, V; Insola, A; Marotta, R. Advanced oxidation processes (AOP) for water purification and recovery. *Catal. Today* **1999**, *53*, 51.

(3) Peranthoner, S.; Centi, G. Wet Hydrogen Peroxide Catalytic Oxidation (WHPCO) of Organic Waste in Agro-Food and Industrial Streams. *Top. Cata*l. **2005**, *33*, 207.

(4) Tukac, V.; Hanika, J. Catalytic Effect of Active Carbon Black Chezacarb in Wet Oxidation of Phenol. *Collect. Czech. Chem. Commun.* **1996**, *61*, 1010.

(5) Stuber, F.; Font, J.; Fortuny, A.; Bengoa, C.; Eftaxias, A.; Fabregat, A. Carbon Materials and Catalytic Wet Air Oxidation of Organic Pollutants in Wastewater. *Top Catal.* **2005**, *33*, 3.

(6) Tatibouët, J. M.; Majesté-Labourdenne, A.; Barrault, J.; Fournier, J. Catalytic Wet Peroxide Oxidation of Phenol on Carbon Supported Iron Catalysts. *Symposium 7 Environ. Catal. 1. End Pipe Technology*, **2001**.

(7) Zazo, J. A.; Casas, J. A.; Mohedano, A. F.; Rodríguez, J. J. Catalytic Wet Peroxide Oxidation of Phenol with a Fe/Active Carbon Catalyst. *Appl. Catal., B* **2006**, *65*, 261.

(8) Mundale, V. D.; Joglekar, H. S.; Kalam, A.; Joshi, J. B. Regeneration of Spent Activated Carbon by Wet Air Oxidation. *Can. J. Chem. Eng*. **1991**, *69*, 1149.

(9) Lücking, F.; Köser, H.; Jank, M.; Ritter, A. Iron Powder, Graphite and Activated Carbon as Catalysts for the Oxidation of 4-chlorophenol with Hydrogen Peroxide in Aqueous Solution. *Water Res*. **1998**, *32*, 2607.

(10) Oliveira, L. C. A.; Silva, C. N.; Yoshida, M. I.; Lago, R. M. The Effect of $H_2$ Treatment on the Activity of Activated Carbon for the Oxidation of Organic Contaminants in Water and the $H_2O_2$ Decomposition. *Carbon* **2004**, *42*, 2279.

(11) Georgi, A.; Kopinke, F. D. Interaction of Adsorption and Catalytic Reactions in Water Decontamination Processes Part I. Oxidation of Organic Contaminants with Hydrogen Peroxide Catalyzed by Activated Carbon. *Appl. Catal., B* **2005**, *58*, 9.

(12) Sandell, E. B. *Colorimetric Determination of Traces of Metals*, Interscience Pubs.: New York, 1959.

(13) Rodríguez-Reinoso, F. The Role of Carbon Materials in Heterogeneous Catalysis. *Carbon* **1998**, *36*, 159.

(14) Stoeckli, H. F. Microporous Carbons and Their Characterization. The Present State-of-the-Art. *Carbon* **1990**, *28*, 1.

(15) Jiang, W.; Tran, T.; Song, X.; Kinoshita, K. Thermal and Electrochemical Studies of Carbons for Li-ion Batteries 1. Thermal analysis of Petroleum and Pitch Cokes. *J. Power Sources* **2000**, *85*, 261.

(16) Radovic, L.; Walker, P.; Jenkis, R. Importance of Carbon Active-Sites in the Gasification of Coal Chars. *Fuel* **1983**, *62*, 849.

(17) Laine, N.; Vastola, F.; Walker, P. Importance of Active Surface Area in Carbon-Oxygen Reaction. *J. Phys. Chem*. **1963**, *67*, 2030.

(18) Coltharp, M.; Hacerman, N. Surface of a Carbon with Sorbed Oxygen on Pyrolysis. *J. Phys. Chem*. **1968**, *72*, 1171.

(19) Welham, N.; Willianms, J. Extended Milling of Graphite and Activated Carbon. *Carbon* **1998**, *36*, 1309.

(20) Moreno-Castilla, C.; Ferro-García, M. A.; Joly, J. P.; Bautista-Toledo, I.; Carrasco-Marín, F.; Rivera-Utrilla, J. Activated Carbon Surface Modifications by Nitric Acid, Hydrogen Peroxide and Ammonium Peroxydisulfate Treatments. *Langmuir* **1995**, *11*, 4386.

(21) Kelemen, S. R.; Freund, H. XPS Characterization of Glassy-Carbon Surfaces Oxidized by $O_2$, $CO_2$ and $HNO_3$. *Energy Fuels* **1988**, *2*, 111.

(22) Gardner, S. D.; Singamsetty, C. S. K.; Booth, G. L.; He, G. Surface Characterization of Carbon Fibers Using Angle-Resolved XPS and ISS. *Carbon* **1995**, *33*, 587.

(23) Estrade-Szwarckopf, H. XPS Photoemission in Carbonaceous Materials: A “Defect” Peak Beside the Graphitic Asymmetric Peak. *Carbon* **2004**, *42*, 1713.

(24) Darmstadt, H.; Roy, C.; Kaliagune, S. ESCA Characterization of Commercial Carbon-Blacks and of Carbon-Blacks from Vacuum Pyrolysis of Used Tires. *Carbon* **1994**, *32*, 1399.

(25) Figueiredo, J. L.; Pereira, M. F. R.; Freitas, M. M. A.; Órfäo, J. J. M. Modification of the Surface Chemistry of Activated Carbons. *Carbon* **1999**, *37*, 1379.

(26) Desimoni, E.; Casella, G. I.; Morone, A.; Salvi, A. M. XPS Determination of Oxygen Containing Functional Groups on Carbon Fiber Surfaces and the Cleaning of These Surfaces. *Surf. Interface Anal.* **1990**, *15*, 627.

(27) Moreno-Castilla, C.; Carrasco-Marín, F.; Maldonado-Hodar, F. J.; Rivera-Utrilla, J. Effects of Non-oxidant and Oxidant Acid Treatments on the Surface Properties of an Activated Carbon with Very Low Ash Content. *Carbon* **1998**, *36*, 145.

(28) Moreno-Castilla, C.; López-Ramón, M. V.; Carrasco-Marín, F. Changes in Surface Chemistry of Activated Carbons by Wet Oxidation. *Carbon* **2000**, *38*, 1995.

(29) Cordero, T.; Rodríguez-Mirasol, J.; Tancredi, N.; Piriz, J.; Vivo, G.; Rodríguez, J. J. Influence of Surface Composition and Pore Structure on Cr(III) Adsorption onto Activated Carbons. *Ind. Eng. Chem. Res.* **2002**, *41*, 6042.

(30) Khalil, L. B.; Girgis, B. S.; Tawfik, T. A. Decomposition of $H_2O_2$ on Activated Carbon Obtained from Olive Stones. *J. Chem. Technol. Biotechnol*. **2001**, *76*, 1132.

(31) Kimura, M.; Miyamoto, I. Discovery of the Activated Carbon Radical $AC^+$ and the Novel Oxidation Reactions Comprising the $AC/AC^+$ Cycle as a Catalyst in an Aqueous Solution. *Bull. Chem. Soc. Jpn*. **1994**, *67*, 2357.

(32) Alnaizy, R.; Akgerman, A. Advanced Oxidation of Phenolic Compounds. *Adv. Environ. Res*. **2000**, *4*, 233.

(33) Zazo, J. A.; Casas, J. A.; Mohedano, A. F.; Gilarranz, M. A.; Rodríguez, J. J. Chemical Pathway and Kinetics of Phenol Oxidation by Fenton's Reagent. *Environ. Sci. Technol.* **2005**, *39*, 9295.

Table 1.- Elemental analysis of activated carbons (wt. %, d.b.)

| Chemical Element | CM | CN | CC |
|---|---|---|---|
| % C | 89.55 | 86.69 | 82.55 |
| % H | 0.67 | 1.00 | 1.56 |
| % N | 0.53 | 0.58 | 1.34 |
| % S | 0.73 | 0.78 | 0.73 |
| % O* | 3.79 | 2.60 | 9.03 |
| % Ashes | 4.73 | 8.35 | 4.79 |

* $\%\,O = 100 - (\%\,C + \%\,H + \%\,N + \%\,S + \%\,Ashes)$

Table 2.- Thermal parameters obtained by TG-DTA in air flow

| SUPPORT | $T_i$ (K) | $T_{15}$ (K) | $T_M$ (K) |
|---|---|---|---|
| CM | 738 | 824 | 865 |
| CN | 672 | 773 | 813 |
| CC | 653 | 771 | 778 |

Table 3.- Porous structure and $pH_{slurry}$ of the activated carbons

| SAMPLE | $S_{BET}$ ($m^2 \cdot g^{-1}$) | $A_{MICRO}$ ($m^2 \cdot g^{-1}$) | $A_{EXT}$ ($m^2 \cdot g^{-1}$) | $V_{TOTAL}$ ($cm^3 \cdot g^{-1}$) | $pH_{slurry}$ |
|---|---|---|---|---|---|
| CM | 1135 | 1023 | 112 | 0.77 | 8.1 |
| CN | 1065 | 903 | 162 | 0.93 | 10.4 |
| CC | 962 | 954 | 8 | 0.44 | 6.2 |
| CN_N | 934 | 841 | 93 | 0.71 | 11.0 |
| CN_HCl | 994 | 882 | 112 | 0.79 | 5.0 |
| CN_HCl_N | 991 | 898 | 93 | 0.73 | 8.3 |

Table 4.- Surface groups distribution obtained from deconvolution of C(1s) and O(1s) XPS regions of the activated carbons.

| | | Surface groups distribution (%) | | |
|---|---|---|---|---|
| **Peak** | **Assessment** | **CM** | **CN** | **CC** |
| C 1s | | | | |
| 284.5 | C=C | 67.6 | 68.0 | 68.1 |
| 286.0 | C–OH; C–O–C | 13.0 | 15.0 | 14.7 |
| 287.1 | C=O | 9.7 | 6.5 | 7.1 |
| 288.5 | COOH; COOC | 3.2 | 3.6 | 3.5 |
| 290.5 | $\pi \rightarrow \pi^*$ | 6.8 | 6.9 | 6.7 |
| O 1s | | | | |
| 530.0 | O–II | 10.7 | 12.2 | 12.9 |
| 531.5 | C=O | 27.5 | 33.9 | 31.8 |
| 532.9 | C–O | 36.8 | 31.8 | 33.6 |
| 534.0 | COOH | 19.6 | 16.9 | 16.3 |
| 536.0 | Adsorbed $H_2O$ | 5.5 | 5.1 | 5.4 |

Table 5.- Assessment of oxygen groups from TPD deconvolution

| SUPPORT | $CO_2$ evolving groups (%) | | | | CO evolving groups (%) | | |
|---|---|---|---|---|---|---|---|
| | CARBOXYLIC | ANHYDRIDE | LACTONE | PYRONE | ANHYDRIDE | PHENOLIC | CARBONYL |
| CM | 100 | ---- | ---- | ---- | ---- | 26.5 | 73.5 |
| CN | 39.5 | 10.0 | 23.0 | 27.5 | 2.4 | 10.7 | 86.9 |
| CC | 63.5 | 21.4 | 15.1 | ---- | 4.5 | 40.7 | 54.8 |

Table 6.- O/C Atomic ratios of the activated carbons.

| SAMPLE | BULK | XPS | TPD |
|---|---|---|---|
| CM | 0.030 | 0.029 | 0.004 |
| CN | 0.020 | 0.046 | 0.019 |
| CC | 0.080 | 0.070 | 0.025 |

Table 7.- First order rate constants for direct $H_2O_2$ decomposition

| SAMPLE | CM | CN | CC |
|---|---|---|---|
| k ($min^{-1}$) | 0.019 | 0.077 | 0.192 |
| $r^2$ | 0.996 | 0.995 | 0.997 |

Table 8.- TPD results of the original and modified CN carbons

| SAMPLE | $CO_2$ evolved ($\mu mol \cdot g^{-1}$) | CO evolved ($\mu mol \cdot g^{-1}$) |
|---|---|---|
| CN | 329.5 | 782.1 |
| CN_N | 43.2 | 228.6 |
| CN_HCl | 145.5 | 714.3 |
| CN_HCl_N | 34.1 | 467.9 |

Table 9.- Catalytic activity results for the original and modified CN carbons

| SAMPLE | $H_2O_2$ Decomposition | | Phenol adsorption | CWPO of phenol | | |
|---|---|---|---|---|---|---|
| | k ($min^{-1}$) | $r^2$ | $X_{TOC}$ (t=240 min) (%) | k ($min^{-1}$) | $r^2$ | $X_{TOC}$ (t=240 min) (%) |
| CN | 0.077 | 0.995 | 56.4 | 0.028 | 0.993 | 90.2 |
| CN_N | 0.065 | 0.998 | 55.0 | 0.021 | 0.991 | 84.4 |
| CN_HCl | 0.069 | 0.999 | 50.6 | 0.027 | 0.993 | 65.2 |
| CN_HCl_N | 0.111 | 0.996 | 60.6 | 0.037 | 0.996 | 74.4 |

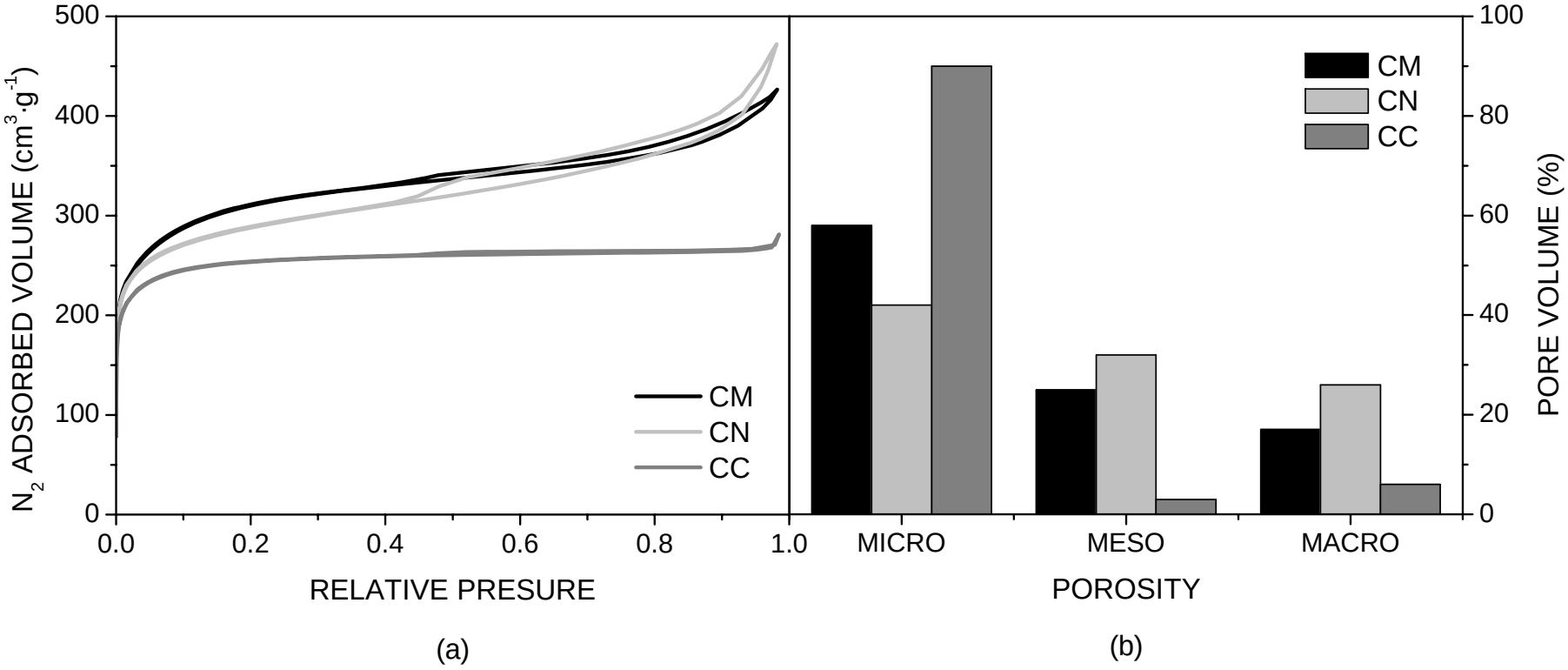


Figure 1.- (a) $N_2$ adsorption-desorption isotherms and (b) pore volume distribution (%) of the activated carbons CM, CN, CC

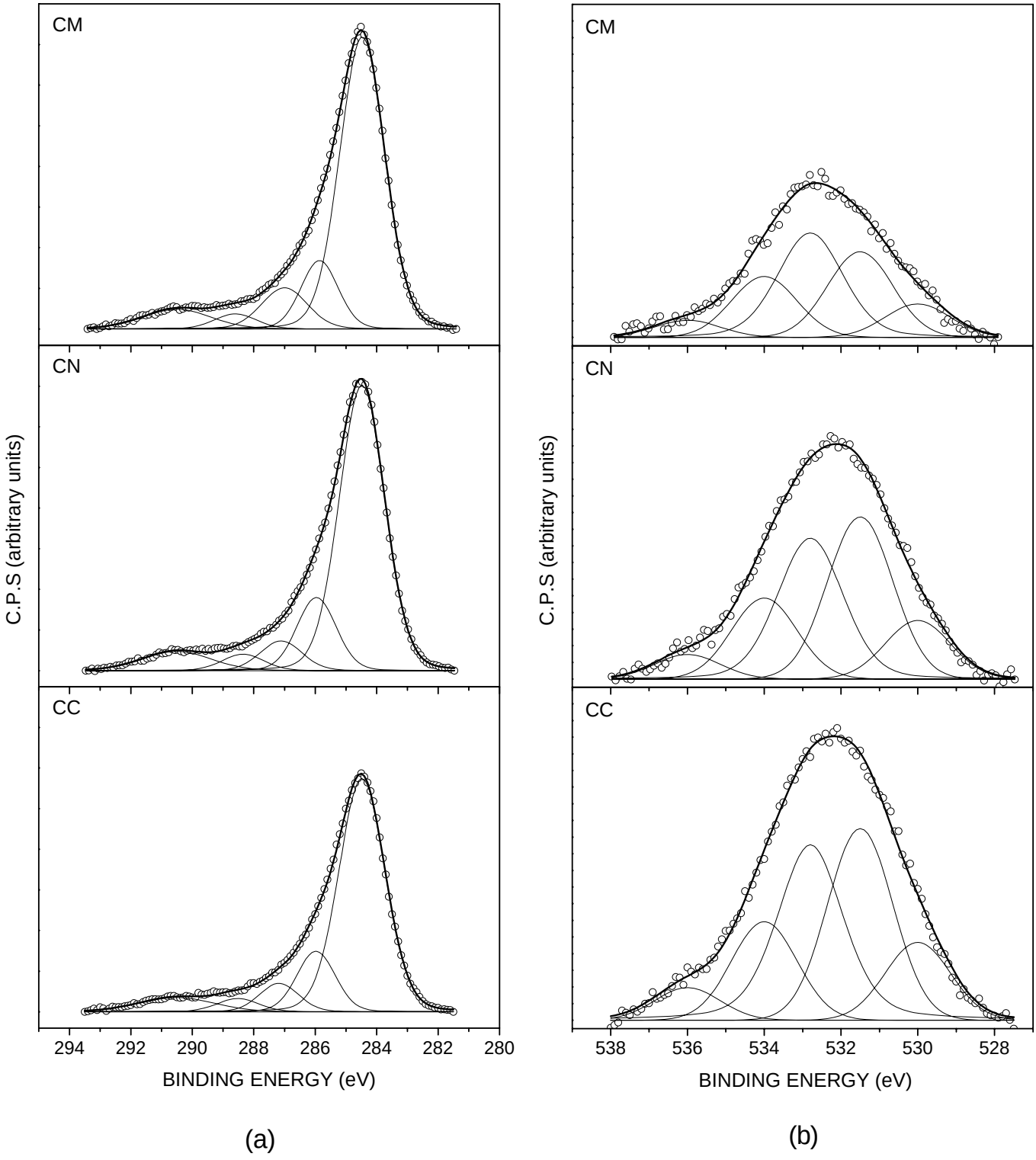


Figure 2.- XPS spectra and deconvolution of the activated carbons. (a) C 1s spectral region, (b) O 1s spectral region

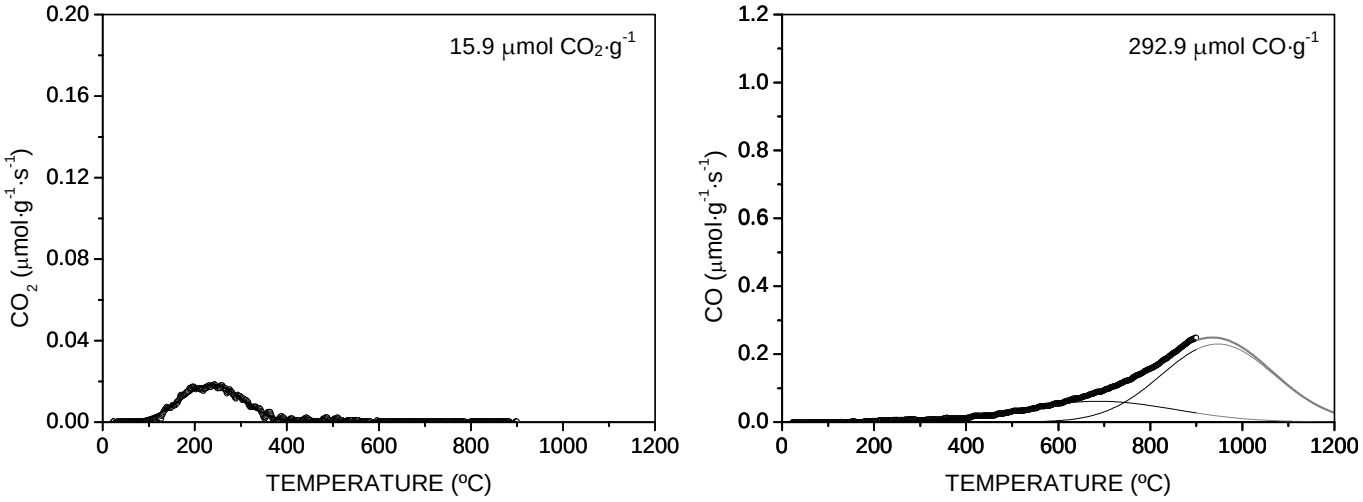


(a)

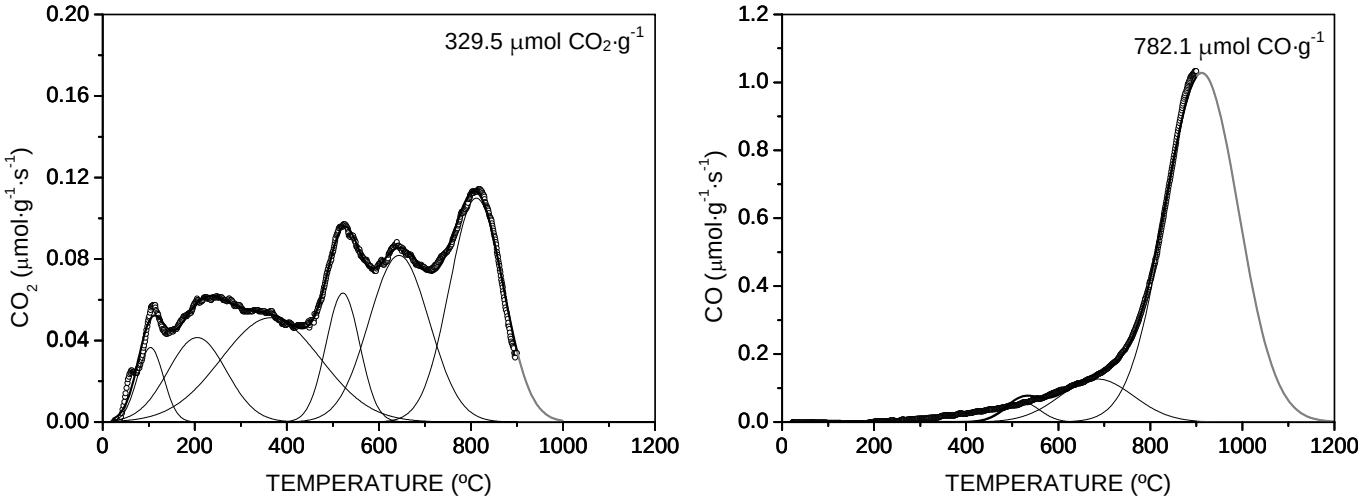


(b)

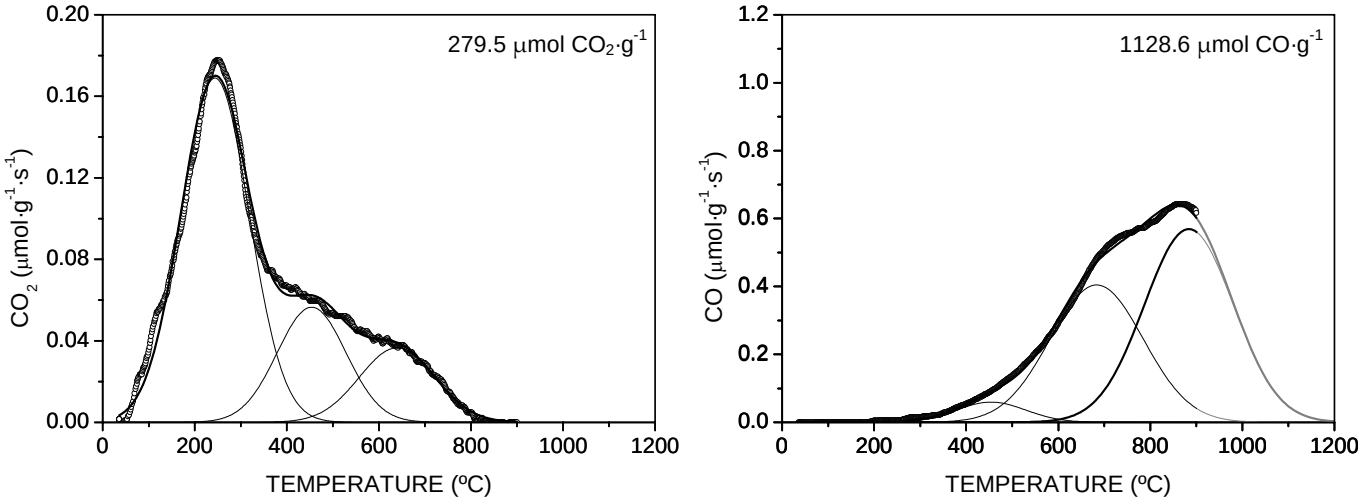


(c)

Figure 3.- TPD curves and deconvolution. (a) CM. (b) CN. (c) CC.

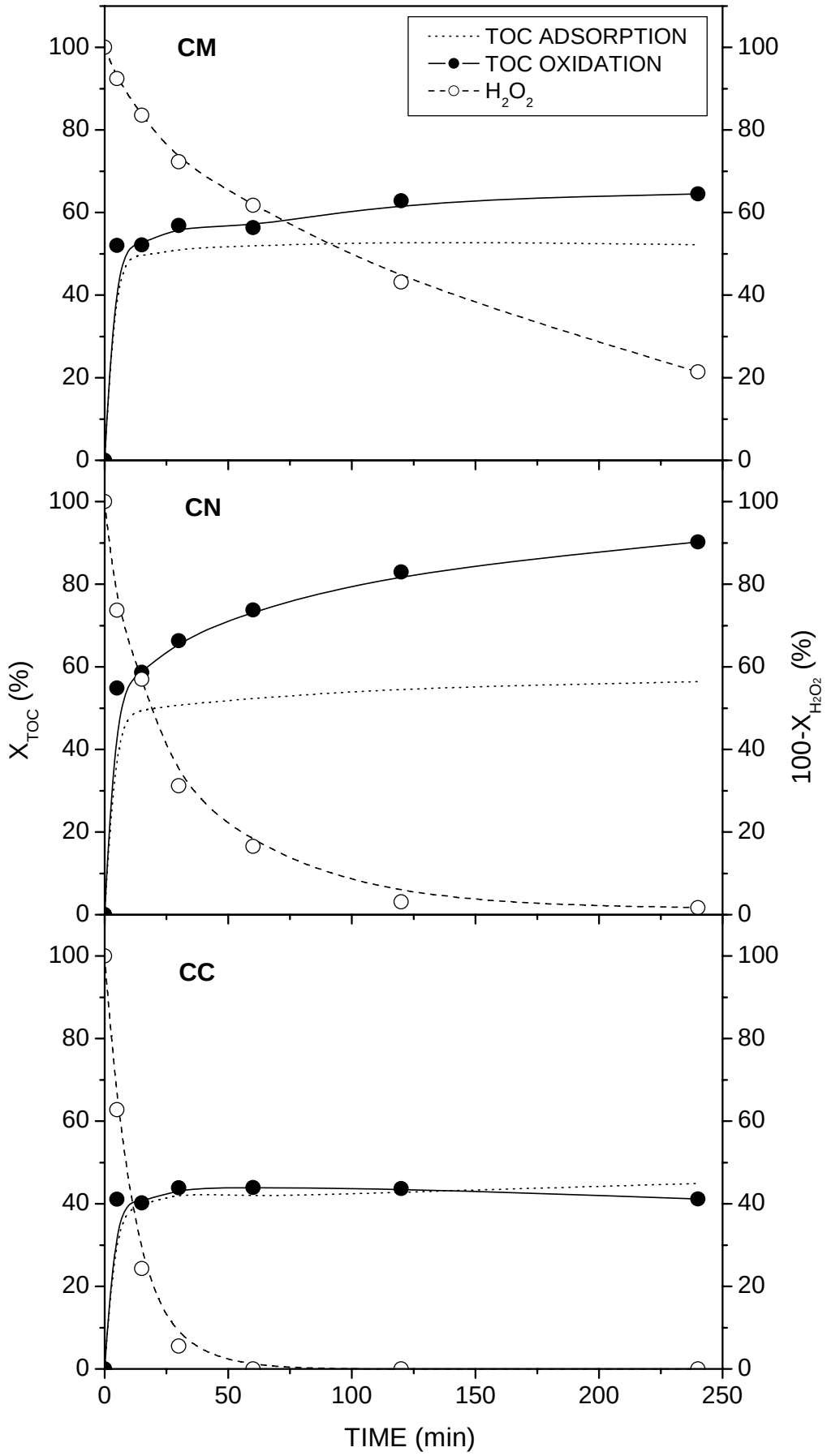


Figure 4.- Conversion-time curves for TOC and $H_2O_2$ in CWPO of phenol.

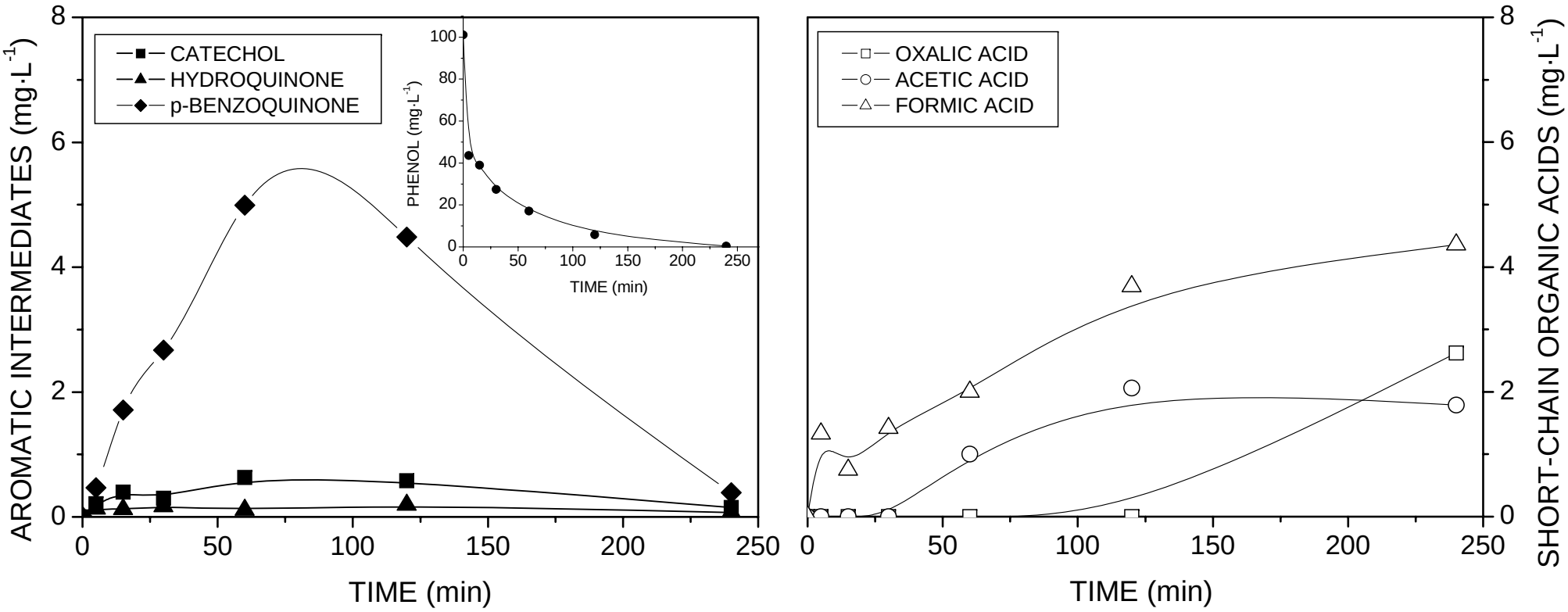


Figure 5.- Evolution of phenol, aromatic intermediates and short organic acids in CWPO of phenol with the CN activated carbon